Continuous Diffuse Electron Scattering from Polymethylene Compounds. A Qualitative Description

Douglas L. Dorset

Molecular Biophysics Department, Medical Foundation of Buffalo, Inc.
73 High Street, Buffalo, New York 14203

(Z. Naturforsch. **32 a**, 1161—1165 [1977]; received June 6, 1977)

The positions of continuous thermal diffuse scattering streaks in electron diffraction patterns of polymethylene chains packing in hexagonal and orthorhombic perpendicular subcells are predicted using the kinematical difference Fourier transform model of Amorós and Amorós. Indications of correlated chain motions are found for the case of the orthorhombic subcell.

Continuous bands of diffusely scattered high energy radiation due to acoustical phonons in crystals have been widely encountered in diffraction experiments — yet they have been often overlooked. Early recognition of their presence in the X-ray diffraction from molecular crystals [1] included a citation of earlier electron diffraction results from anthracene reported by Charlesby et al. [2]. In these studies it was recognized that the continuous thermal diffuse scattering from molecular crystals is somehow related to the Fourier transform of the constituent molecule in the crystal, consistent with its projection in a given crystal orientation. An elegant qualitative description of the continuous scattering was developed by Amorós and Amorós [3] using the molecular Q-function of Hosemann and Bagchi [4], which is the autocorrelation function of a single molecule.

For a case of one molecule per unit cell, the whole Q-function of the thermally agitated unimolecular crystal is given [3]:

$$Q(\boldsymbol{r}) = \bar{Q}_{\mathrm{mole_T}}(\boldsymbol{r})^* z_{\mathrm{cr}}(\boldsymbol{r}) + Q_{\mathrm{mole_0}}(\boldsymbol{r}) - \bar{Q}_{\mathrm{mole_T}}(\boldsymbol{r}) = P_{\mathrm{T}}(\boldsymbol{r}) + Q_{\mathrm{mole_0}}(\boldsymbol{r}) - \bar{Q}_{\mathrm{mole_T}}(\boldsymbol{r})\,. \quad (1)$$

Here $\bar{Q}_{\mathrm{mole_T}}(\boldsymbol{r})$ represents the Q-function of an average molecule. When it is convoluted with the space lattice function $z_{\mathrm{cr}}(\boldsymbol{r})$, it generates the Patterson function $P_{\mathrm{T}}(\boldsymbol{r})$ of the thermally disordered crystal. The term $Q_{\mathrm{mole_0}}(\boldsymbol{r})$ is similarly the Q-function for a molecule at rest. The Fourier transform of the Patterson function in (1) gives the spot pattern intensities for the crystal whereas the transform of $Q_0 - \bar{Q}_{\mathrm{T}}$ describes the continuous scattering intensity due to thermal agitation of molecules, i.e.

$$I(\boldsymbol{r}^*) = I_{\mathrm{mole}}(\boldsymbol{r}^*)\,|D|^2 Z_{\mathrm{cr}}(\boldsymbol{r}^*) + I_{\mathrm{mole}}(\boldsymbol{r}^*) \cdot (1 - |D|^2)\,. \quad (2)$$

Here $|D|^2$ represents the squared Debye-Waller factor and $Z_{\mathrm{cr}}(\boldsymbol{r}^*)$ is the reciprocal lattice function. In the case of a unit cell with two molecules, the Q-function becomes [3]:

$$Q(\boldsymbol{r}) = Q_1 + Q_2 - \bar{Q}_1 - \bar{Q}_2 + P_{\mathrm{T}}(\boldsymbol{r})$$

where the subscripts refer to separate molecules. The motions of the single molecules are assumed to be uncorrelated and thus their individual contributions to the continuous scatter are considered separately and additively with no regard to space group symmetry, i.e. they scatter incoherently. The intensity of the diffuse scattering is calculated from the second part of (2), called the difference Fourier transform or DFT [3]. Its form is similar to the empirical expression for diffuse scattering found by Charlesby et al. [2].

Diffuse streaks have been seen by us in spot electron diffraction patterns from polymethylene compounds, particularly if the crystals are multilamellar. A simple example of this is shown in Fig. 1, an $hk0$ electron diffraction pattern from the hexagonal polymorph of 1,2-dimyristoyl *sn* glycerophosphocholine [5]. In this pattern the (100) spots are connected by the continuous bands. More complex arrays of non-radial diffuse streaks are seen in $hk0$ diffraction patterns from multilamellar crystals of orthorhombic n-hexatriacontane (Figure 2). The same diffuse streaks are more discernable in a published polyethylene electron diffraction pattern, representing the same (001) projection of the $0_\perp$ methylene subcell (see Fig. 3a in Reference [6]).

Reprint requests to Dr. Douglas L. Dorset, Medical Foundation of Buffalo, Inc., 73 High Street, Buffalo, New York 14203, USA.

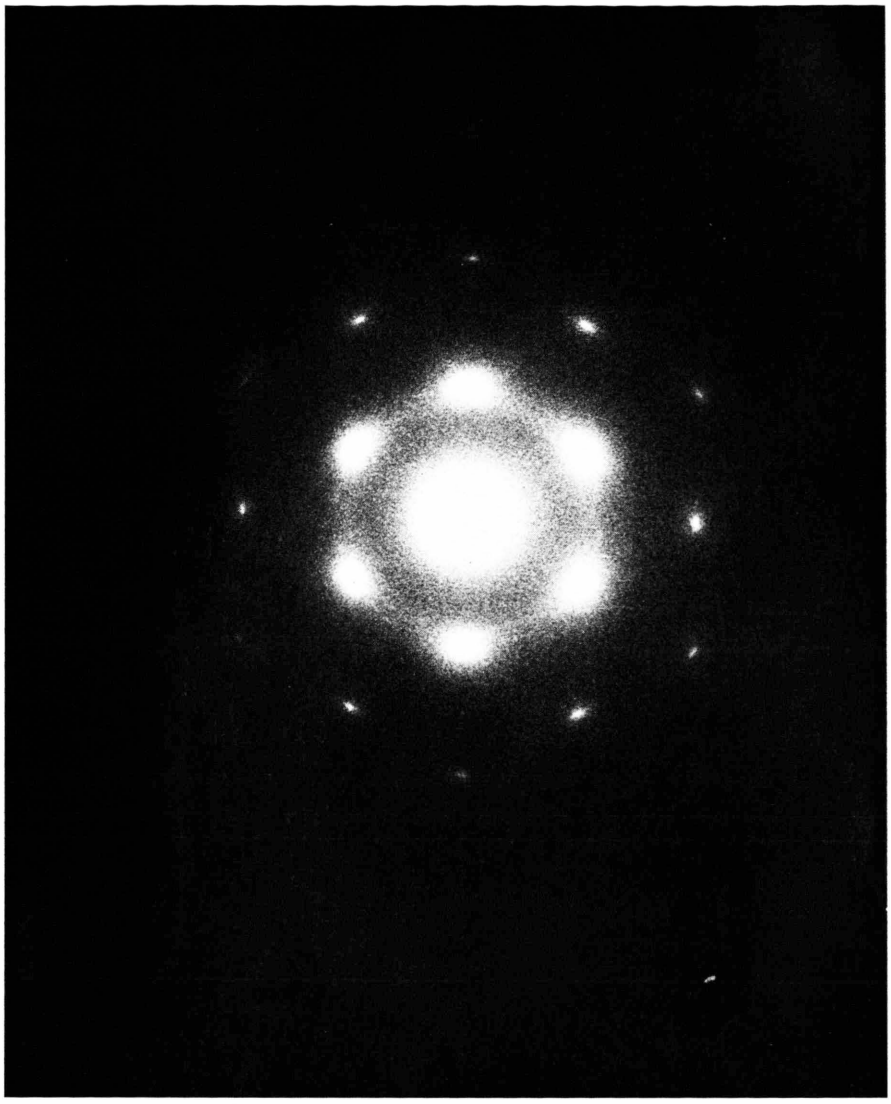

Fig. 1. Electron diffraction pattern ($hk0$) from hexagonal methylene subcell. Sample: 1,2-dimyristoyl *sn* glycerophosphocholine. Accelerating voltage 100 kV.

Qualitative interpretation of these observed continuous bands was made on the basis of kinematical diffraction theory and the DFT approach of Amorós and Amorós[3]. The hexagonal subcell (Fig. 1) affords the simplest example since there is only one long chain per unit cell[7,8]. DFT calculations were carried out using

$$I_{\mathrm{DFT}} = |F_{hk0}|^2 \{1 - \exp(-\tfrac{1}{2} B |\boldsymbol{r}^*|^2)\} \qquad (3)$$

where the structure factor F_{hk0} is calculated with the expression for diffraction from a free rotor given by Vainshtein[9] and used earlier by us[7,8] in our quantitative description of the hexagonal subcell. Instead of only calculating F_{hk0} at integral values of Miller indices the structure factors were evaluated at intervals $h, k = 1/4$ in order to map a continuous scattering function. The value of B was arbitrarily set at 6.0 Å^2. The good agreement of predicted diffuse continuous scattering with observed diffraction is shown by a comparison of Fig. 3 with Figure 1.

It should be pointed out here that this type of continuous scatter can be confused with the diffuse ring from the amorphous carbon layer of the sup-

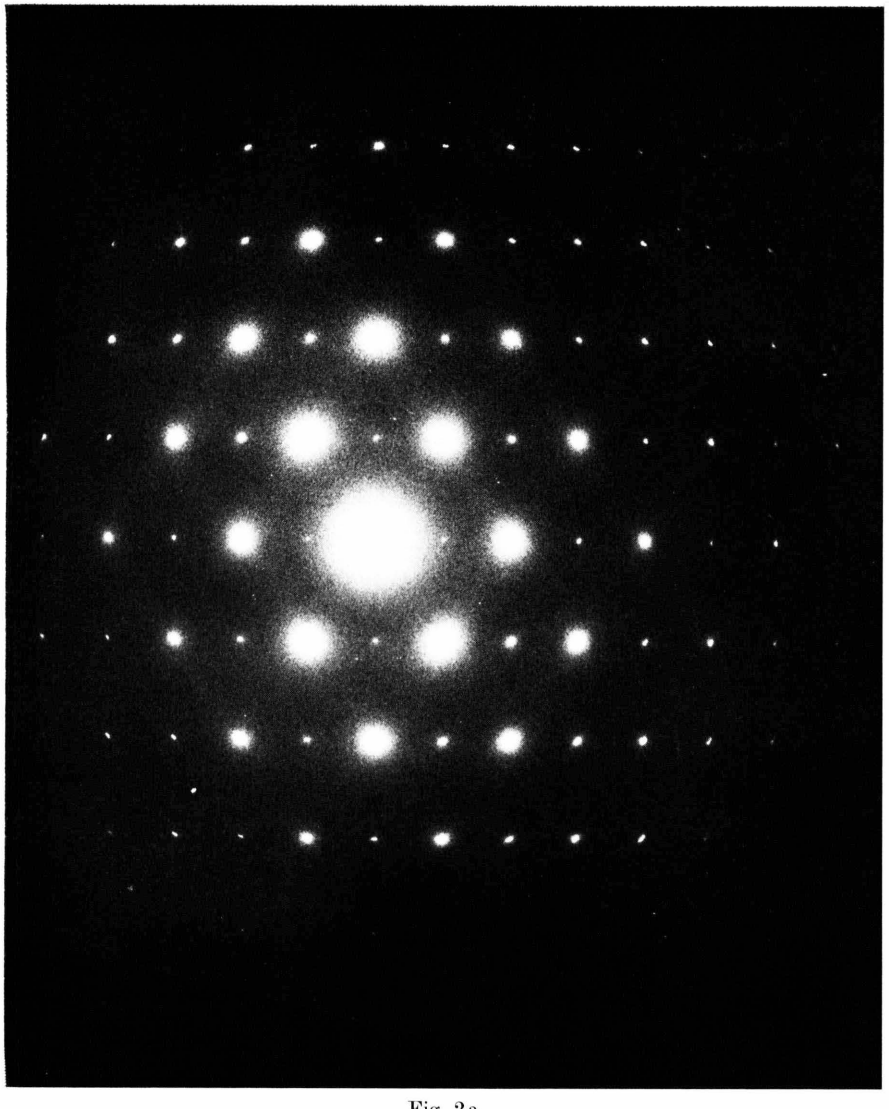

Fig. 2a

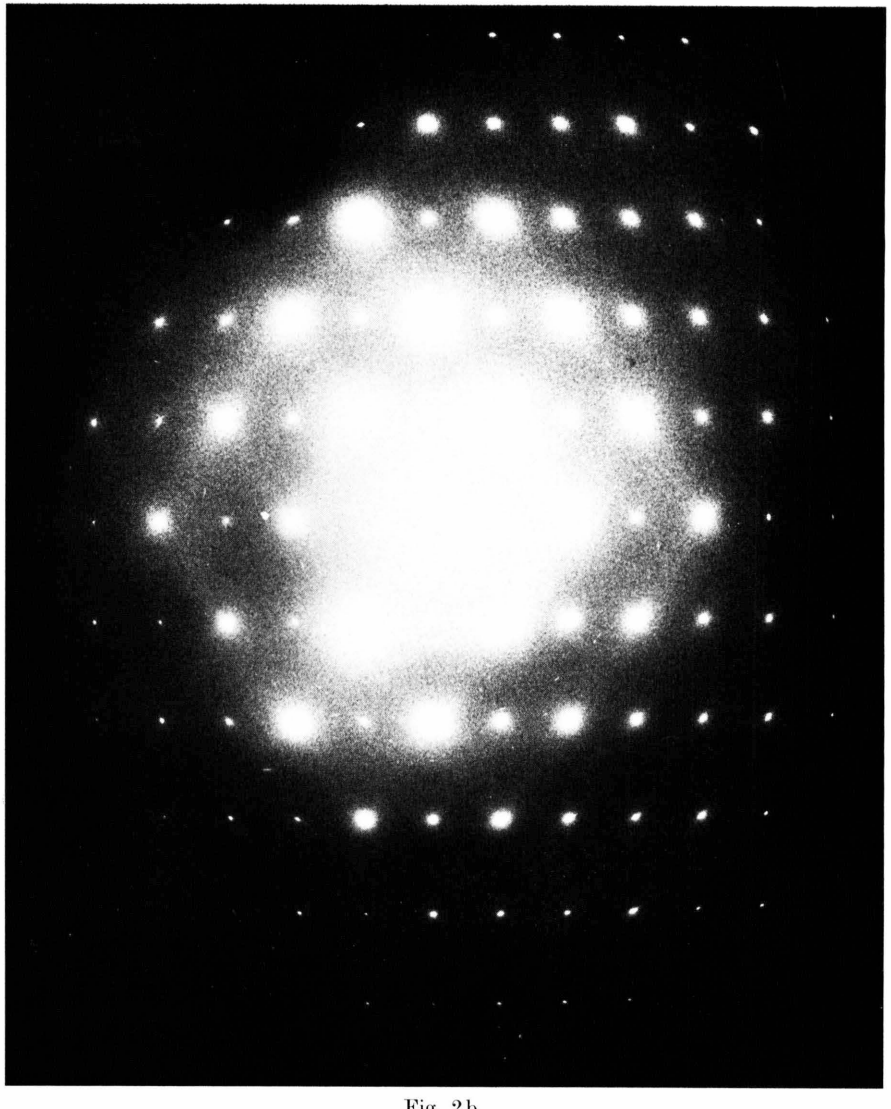

Fig. 2b

Fig. 2. Electron diffraction pattern ($hk0$) from orthorhombic perpendicular ($0_\perp$) methylenesubcell. Sample: n-hexatriacontane. Accelerating voltage 80 kV.

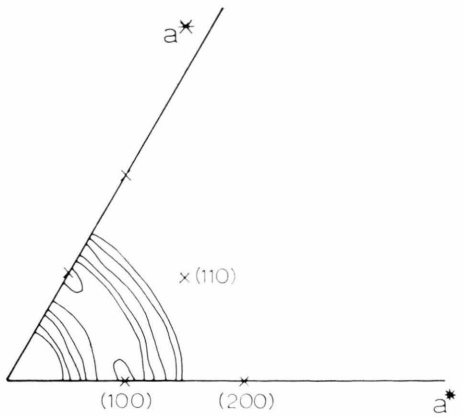

Fig. 3. Difference Fourier transform (DFT) of long chain in hexagonal methylene subcell, (001) projection. Positions of major Bragg peaks indicated. $B = 6$ Å^2. Most intense contour represents 0.16 (I_{100}) at $B = 0$ Å^2.

port film of the electron microscope grid, even as it has been for more complex diffuse patterns from polyethylene[6]. The center of intensity for the first ring of amorphous carbon scattering should occur about (4.8 Å)$^{-1}$ in reciprocal space[10] whereas the thermal diffuse scattering from the hexagonal methylene subcell connects (100) spots at (4.2 Å)$^{-1}$. The first diffuse ring from a poly(vinylformal) grid support film is measured at (4.7 Å)$^{-1}$.

The interpretation of continuous thermal scattering from the $0_\perp$ methylene subcell is less straightforward. The unit cell contains two molecules[11], and using the criterion of incoherence due to uncorrelated motion of neighboring chains[3], their contribution must be considered separately i.e. as $\sum |F_{hk0}|^2$ in (3) above. A DFT map calculated on this basis, again using $B = 6$ Å^2, is shown in Figure 4. As expected, the (200) reflection is linked to the (110) but the band does not continue as observed, all the way to (020). Moreover, appreciable diffuse intensity is predicted around the forbidden (300) spot. (The appearance of this spot in Fig. 2 is due to multiple elastic scattering in multilayers[12,13].) Higher order streaks also are not predicted.

A more satisfactory explanation of the observed diffuse bands is found if the motions of adjacent long chains are assumed to be correlated, i.e. if F_{hk0} in (3) is calculated for the whole unit cell rather than one molecule. This is illustrated by comparing Fig. 5 with Figure 2. The description of the continuous scattering is not complete, however. Careful examination of Fig. 2 reveals that streaks perpendi-

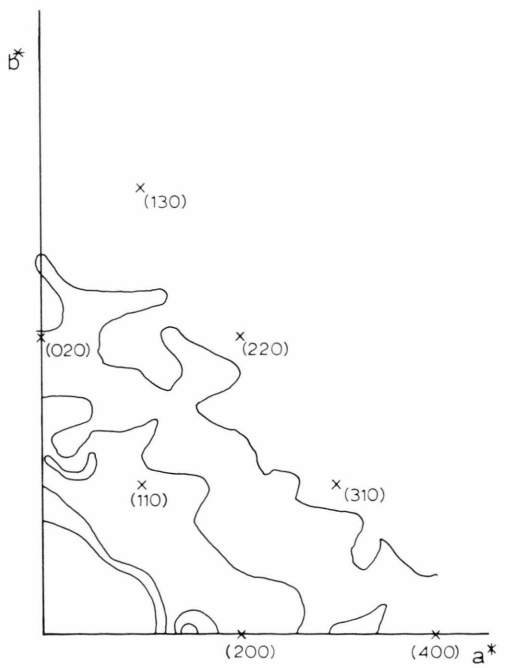

Fig. 4. DFT of long chains in $0_\perp$ methylene subcell assuming chain motions are uncorrelated, (001) projection. Positions of major Bragg peaks indicated. $B = 6$ Å^2. Most intense contour represents 0.16 (I_{110}) at $B = 0$ Å^2.

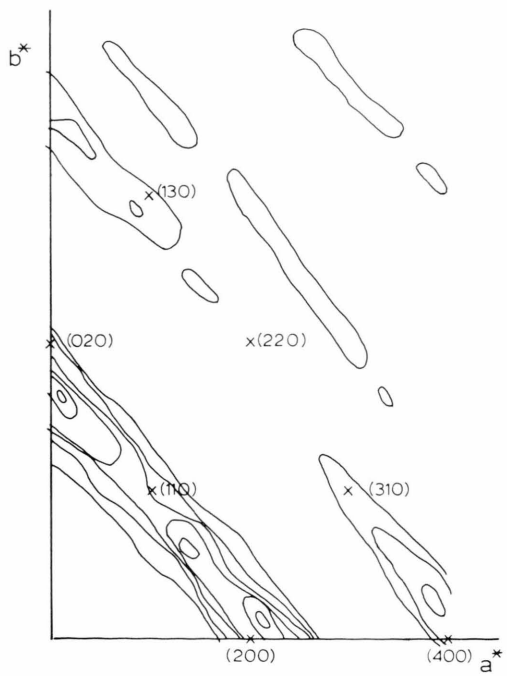

Fig. 5. DFT of long chains in $0_\perp$ methylene subcell assuming correlated chain motions, (001) projection. Positions of major Bragg peaks indicated. $B = 6$ Å^2. Most intense contour represents 0.24 (I_{110}) at $B = 0$ Å^2.

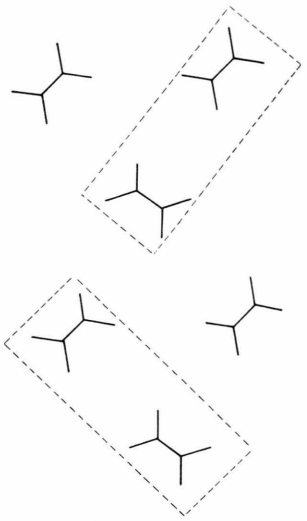

Fig. 6. $0_{\perp}$ methylene subcell. Proposed bimolecular clusters related by mirrorplane are indicated by dashed box outline.

cular to the predicted intensity bands are apparent in the total diffraction pattern. This phenomenon might be explained if the coupled motion of adjacent chains could be restricted to small clusters — e.g. bimolecular clusters related by mirror symmetry as shown in Figure 6.

The thermal streak patterns are obviously related to the structure of the molecules in (001) projection since the streaks are elongated in a reciprocal direction corresponding to the normal to the zig-zag chain plane, as was also found for dicarboxylic acids[3]. This is consistent with expected modulation of the scattering by the molecular shape function. As stated by Doyle[14] in his development of n-beam dynamical diffraction theory for non-continuous thermal diffuse scattering around Bragg peaks, the continuous streaks described here are not dependent upon dynamical effects-although their intensity may be stronger than expected kinematically. Thus, the use of $B = 6$ Å^2 in the calculations above, which only magnifies the presence of given streaks, may not be an accurate indication of the real average temperature factor. For example, $B = 3$ Å^2 was used in n-beam dynamical corrections to spot intensity data from the paraffin[13].

Research supported by NIH Grant No. GM-21047 awarded by the National Institute of General Medical Science.

[1] K. Lonsdale and H. Smith, Proc. Roy. Soc. London **A 179**, 8 [1942].
[2] A. Charlesby, G. I. Finch, and H. Wilman, Proc. Phys. Soc. **51**, 479 [1939].
[3] J. L. Amorós and M. Amorós, Molecular Crystals: Their Transforms and Diffuse Scattering. Wiley, New York 1968.
[4] R. Hosemann and S. N. Bagchi, Acta Crystallogr. **5**, 749 [1952].
[5] D. L. Dorset, Biochim. Biophys. Acta **380**, 257 [1975].
[6] K. Kobayashi and K. Sakaoku, Lab. Invest. **14**, 1097 [1965].
[7] D. L. Dorset, Chem. Phys. Lipids **13**, 133 [1974].
[8] D. L. Dorset, Chem. Phys. Lipids **20** (in press).
[9] B. K. Vainshtein, Sov. Phys. — Crystallogr. **8**, 127 [1963].
[10] J. Gjønnes, Acta Crystallogr. **12**, 976 [1959].
[11] P. W. Teare, Acta Crystallogr. **12**, 294 [1959].
[12] J. M. Cowley, A. L. G. Rees, and J. A. Spink, Phys. Soc. **A 64**, 604 [1951].
[13] D. L. Dorset, Acta Crystallogr. **A 32**, 207 [1976].
[14] P. A. Doyle, Acta Crystallogr. **A 25**, 569 [1969].